Macromolecules

pubs.acs.org/Macromolecules Article

Self-Healable Acrylic-Based Covalently Adaptable Networks

Siyang Wang, Lei Li, Qianhui Liu, and Marek W. Urban*

Cite This: *Macromolecules* 2022, 55, 4703–4709 Read Online

ACCESS | Metrics & More | Article Recommendations | Supporting Information

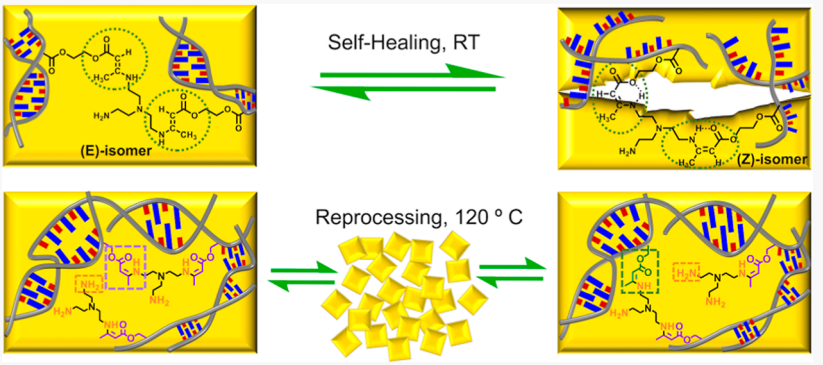

ABSTRACT: Combining autonomous self-healing and reprocessing in one material offers an extended life span and enables shape configuration changes. We developed commodity poly((2-acetoacetoxy)ethyl methacrylate/methyl methacrylate/*n*-butyl acrylate) [p(AAEMA/MMA/nBA)] copolymer networks that are capable of both self-healing without intervention as well as reprocessing. The thermoplastic p(AAEMA/MMA/nBA) was obtained by copolymerizing (2-acetoacetoxy)ethyl methacrylate (AAEMA), methyl methacrylate (MMA), and *n*-butyl acrylate (nBA), followed by cross-linking with tristriaminoethyl amine (TREN) to form covalently adaptable networks (CANs). This copolymer network exhibits self-healability under ambient conditions and reprocessibility by compression molding at 120 °C. Using an array of thermo-mechanical and spectroscopic tools, these studies show that reprocessibility is achieved by the exchange reactions of dynamic cross-links, whereas self-healing is facilitated by the recovery of energetically favorable inter-chain van der Waals interactions accompanied by the reversible $E \rightleftharpoons Z$ isomerization of the C═C bonds in vinylogous urethane moieties of the network.

INTRODUCTION

Self-healing is the ability of materials to autonomously recover from physical damage. The general approaches to self-healing have utilized physical and chemical processes or a combination thereof. They include but are not limited to covalent bond reformation[1−5] and dynamic supramolecular chemistry,[6−9] encapsulation of reactive compounds,[10] or incorporation of superparamagnetic nanoparticles.[11] The use of abundant van der Waals (vdW) interactions is particularly attractive because it does not require elaborate chemical modifications. While the primary goal for developing self-healing materials is to maintain their properties and useful functions, the emerging new class of synthetic materials that resemble enzymatic cleavage of linkers in biological systems are covalently adaptive networks (CANs).[12−14] Their main features are exchangeable covalent bonds facilitating reprocessibility that upon cleavage reshuffle, leading to the recovery of initial or creation of new properties.[13,15] These exchange reactions may be triggered by temperature,[15−17] light,[18,19] pH,[20] oxidation−reduction,[21,22] or other stimuli.[14,23,24] The unique feature of CANs is their versatility of being embedded into an array of polymer networks either by covalent bonding or as additives.

Combining autonomous repairs without intervention under ambient conditions and the ability of reprocessing into a new material is particularly attractive because it prolongs functionality as well as offers an option of reprocessing when new shape reconfigurations are desired. In these studies, we developed self-healable acrylic-based copolymers that recover and maintain mechanical properties upon mechanical damage as well as are capable of on-demand reprocessing.

RESULTS AND DISCUSSION

Inspired by the recent discovery in which vinylogous urethane CANs capable of associative transamination exchange reactions were utilized to achieve reprocessibility,[25] we copolymerized the monomer containing cross-linkable β-ketoester functional groups with commodity acrylic monomers to enhance vdW

Received: April 13, 2022
Revised: May 16, 2022
Published: June 3, 2022

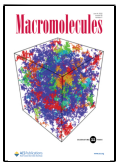

https://doi.org/10.1021/acs.macromol.2c00739
Macromolecules 2022, 55, 4703−4709

Scheme 1. Synthesis of p(AAEMA/MMA/nBA) CANs; (A) RAFT Polymerization of p(AAEMA/MMA/nBA) Prepolymer and End-Group Removal; (B) Cross-Linking of p(AAEMA/MMA/nBA) Using TREN in a 2:1 Molar Ratio

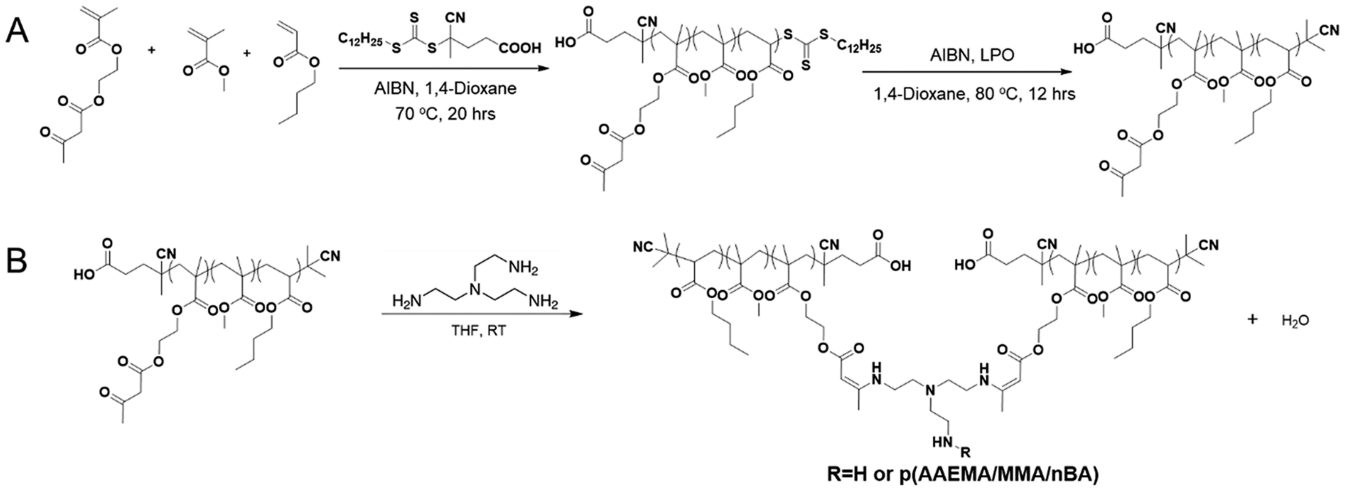

interactions that facilitate self-healing.[9] This integration was achieved by reversible addition−fragmentation chain transfer (RAFT) polymerization of (2-acetoacetoxy)ethyl methacrylate (AAEMA), methyl methacrylate (MMA), and *n*-butyl acrylate (nBA) to form autonomous self-healable and reprocessable poly((2-acetoacetoxy)ethyl methacrylate/methyl methacrylate/*n*-butyl acrylate) [p(AAEMA/MMA/nBA)] CANs.

Scheme 1A illustrates statistical RAFT copolymerization of the p(AAEMA/MMA/nBA) prepolymer containing β-ketoester groups as side chains capable of cross-linking by primary amines. While detailed characterization of each step is provided in the Supporting Information (Figures S1−S4, Table S1), the final step in Scheme 1A illustrates the end-group removal. The product of this reaction p(AAEMA/MMA/nBA) (AAEMA/MMA/nBA = 5.4/44.6/50.0 monomer molar ratio) was cross-linked with tristriaminoethyl amines (TREN) to form p(AAEMA/MMA/nBA) CANs (AAEMA/TREN = 2:1 molar ratio), shown in Scheme 1B.

Figure 1A1,A2 illustrates cross-link exchange reactions involved in the reprocessibility as well as inter-digitated inter-chain vdW interactions, facilitating self-healing of p(AAEMA/MMA/nBA) CANs. The initial cross-linking is formed through condensation reaction between β-ketoesters on AAEMA side groups and the primary amines of the TREN cross-linker. The presence of dynamic cross-links and reactive primary amines facilitates associate exchange reactions resulting in newly formed cross-links as well as the release of amine groups for further reactions. This cross-link exchange allows the network to retain cross-link density through transamination reactions without depleting mechanical properties. These thermal exchange reactions require no catalyst, but not surprisingly, the reactive group stoichiometric balance is of vital importance to ensure the availability of free amines for efficient network reorganizations.[13] At the same time, self-healing is achieved by copolymerization of MMA and nBA monomers forming "key-and-lock" topologies between neighboring chains when MMA/nBA monomer molar ratios are in the self-healing range.[9] The use of dipolar interactions eliminates chemical and physical alterations and enables multiple recoveries without external intervention.[26] Although ideally alternating MMA/nBA sequences are desired, semi-batch programmed monomer feeding will enhance the amount of alternating sequences.[27]

Figure 1B illustrates optical images of reprocessing of the original (solvent-cast unprocessed) p(AAEMA/MMA/nBA) CANs that were mechanically destroyed into smaller pieces, followed by compression molding at 120 °C to yield homogenous films. This process was repeated four times and after each step was characterized in the same manner. As shown in Figure 1C1,C2, the storage modulus of the original films is ∼3.04 GPa at −60 °C (C1), and the glass transition temperature (T_g) is ∼45.5 °C (C2). The absence of perceptible changes in the storage modulus and T_g, also reflected by unchanging tan δ peak positions after multi-reprocessing, indicates recovery of thermo-mechanical properties and retention of the network mechanical integrity. Junction densities (ν_j) and stored entropy (ΔS_s) of the original and reprocessed specimens determined from viscoelastic length transitions[28,29] also show no changes (Table S2), indicating no loss of cross-links during reorganization. Assuming alternating distributions of monomeric units, for the AAMEMA/PMMA/nBA molar ratio of 5.4/44.6/50, AAEMA units are expected to be separated by about ∼28 Å long MMA/nBA units (assuming a fully extended chain and a C−C bond length of 1.6 Å). Under these conditions, and assuming that the TREN's three amine arms are about ∼4.8-5.0 Å long, reactions of the primary amines of TREN and β-ketoesters of AAEMA will predominately form inter-chain cross-linking. Thus, the spatial distribution of AAEMA is expected to be about ∼15 Å apart. On the other hand, the concentration of chemical cross-links per volume will remain unchanged during reprocessing as long as one reactive amine per cross-link is maintained over reprocessing cycles (Figure 1A). The initial cross-link density, although, will depend upon the AAEMA to MMA/nBA molar ratio. For these networks, the tensile strain and the maximum stress at break values are retained at ∼91 and ∼97% after four ($R \times 4$) cycles. The cross-links are thermally stable after $R \times 4$ cycles up to ∼250 °C (Figure S5); the weight loss after 180 min at 120 °C is ∼3% (Figure S6), which is also supported by attenuated total reflectance (ATR) Fourier transform infrared (FTIR) analysis in the C═O/C═C region of the original and reprocessed p(AAEMA/MMA/nBA) CANs (Figure S7).

Autonomous self-healing was conducted under ambient conditions ($T \sim 22$ °C; RH ∼ 34%) on original and $R \times 4$ processed films. Optical images of self-healable p(AAEMA/

https://doi.org/10.1021/acs.macromol.2c00739
Macromolecules 2022, 55, 4703−4709

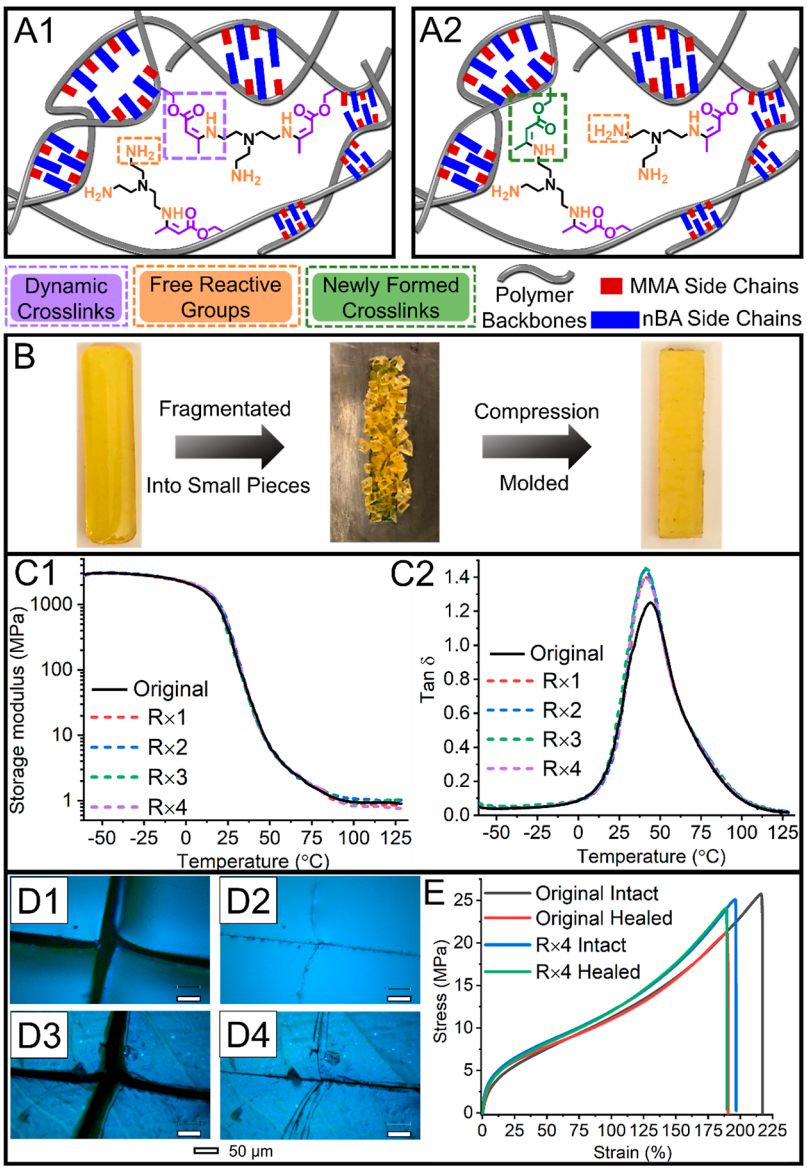

Figure 1. (A1−A2) Schematic illustration of p(AAEMA/MMA/nBA) CANs containing dynamic cross-links that participate in transamination exchange reactions as well as inter-digitated inter-chain topologies facilitated by MMA and nBA repeating units; (B) mechanical and thermal reprocessing of p(AAEMA/MMA/nBA) CANs; overlayed storage modulus (C1), and tan δ (C2) curves obtained from DMA measurements; (D1−D4) optical images of original (solvent-cast unprocessed) and reprocessed p(AAEMA/MMA/nBA) CANs: (D1) original-damaged, (D2) original-self-healed, (D3) reprocessed over four cycles ($R \times 4$), damaged, and (D4) $R \times 4$-self-healed. (E) Stress−strain curves of intact and self-healed specimens after 24 h for original and after four times processing.

MMA/nBA) CANs are shown in Figure 1D1−D4. Damaged films (Figure 1D1) self-heal under ambient conditions within 24 h, and self-healing is maintained after four reprocessing cycles, as illustrated by the optical images of damaged (Figure 1D3) and self-healed (Figure 1D1−D4) specimens. As characterized by tensile measurements of intact and self-healed specimens, recovery of mechanical properties after self-healing is shown in Figure 1E. The original p(AAEMA/MMA/nBA) CANs exhibit the tensile strain of ∼215% with the maximum stress at break ∼25.7 MPa, which is recovered upon self-healing at ∼91 and ∼83%, respectively. Furthermore, reprocessed $R \times 4$ films retain both tensile strain and maximum stress at break recoveries of ∼96 and ∼95% upon self-healing.

The perturbation induced by the damage-repair cycle provides an opportunity for determining molecular events that govern self-healing. ATR FT-IR measurements were used to analyze the damage-repair cycle of original and $R \times 4$ p(AAEMA/MMA/nBA) CANs. While Tables S3 and S4 summarize vibrational bands sensitive to the damage-repair cycle, the characteristic bands at 1600 and 1655 cm^{-1} attributed to C═C and N−H groups of vinylogous urethanes shown in Figure 2 ($R \times 4$) are retained. Furthermore, the intensity of the band at 1600 cm^{-1} due to C═C stretching vibrations increases. This observation raises the question of why the intensity of this band in the original (intact) (Figure 2A1) and ($R \times 4$) (Figure 2B1) specimens increases upon mechanical damage and returns to the same intensities after self-healing (Figure S8). After all, small dipole moment changes of the C═C stretching vibrations are usually reflected in weak IR intensities, thus suggesting either depolymerization or conformational changes in the vicinity of the C═C bonds.

https://doi.org/10.1021/acs.macromol.2c00739
Macromolecules 2022, 55, 4703−4709

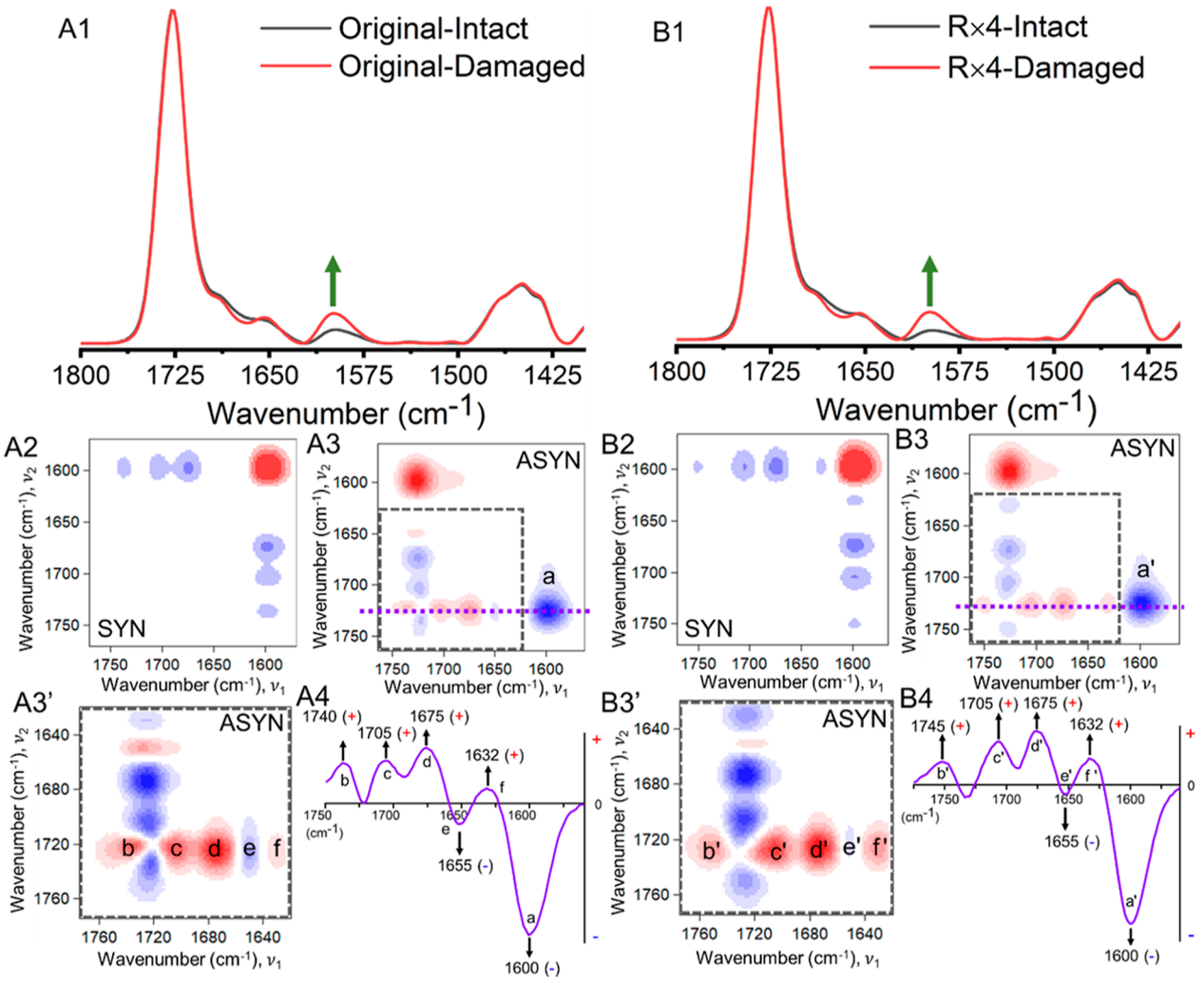

Figure 2. ATR FT-IR spectra and 2D correlation spectroscopic (2D-COS) analysis of original and reprocessed p(AAEMA/MMA/nBA) CANs before and after damage. (A1) Overlayed ATR FT-IR spectra of intact and damaged original p(AAEMA/MMA/nBA) CANs; (A2) synchronous 2D-COS of original p(AAEMA/MMA/nBA) CANs before and after damage in the 1775−1560 cm^{-1} region; (A3) asynchronous 2D-COS of original p(AAEMA/MMA/nBA) CANs before and after damage in the 1775−1560 cm^{-1} region; (A3′) zoomed-in asynchronous 2D-COS of original p(AAEMA/MMA/nBA) CANs before and after damage in the 1765−1620 cm^{-1} region; (A4) correlation slicing profile of asynchronous 2D-COS of original p(AAEMA/MMA/nBA) CANs before and after damage at 1725 cm^{-1}; (B1) overlayed ATR FT-IR spectra of intact and damaged p(AAEMA/MMA/nBA) CANs after being reprocessed over four cycles ($R \times 4$); (B2) synchronous 2D-COS of $R \times 4$ before and after damage in the 1775−1560 cm^{-1} region; (B3) asynchronous 2D-COS of $R \times 4$ before and after damage in the 1775−1560 cm^{-1} region; (B3′) zoomed-in asynchronous 2D-COS of $R \times 4$ before and after damage in the 1765−1620 cm^{-1} region; (B4) correlation slicing profile of asynchronous 2D-COS of $R \times 4$ before and after damage at 1725 cm^{-1}.

DMA analysis (Figure 1C1,C2) rules out depolymerization because the storage modulus, tan δ, ν_j, and ΔS_s values remain unchanged after $R \times 4$ cycles, and the C═C intensities return upon self-healing (Figure S8). However, if the C═C bond is able to twist or rotate, as documented in the literature,[30] conformational changes will be reflected in the intensity changes.

To examine if indeed conformational changes during damage repair are responsible for this behavior, two-dimensional correlation spectroscopic (2D-COS) analysis was employed to analyze ATR FT-IR spectra.[31,32] This approach enables resolving dynamic changes during damage-repair perturbation of original and $R \times 4$ p(AAEMA/MMA/nBA) CANs. Figure 2A2 through B4 show synchronous (SYN) and asynchronous (ASYN) 2D-COS analysis of ATR FT-IR spectra of intact (ν_1) and damaged (ν_2) states that are correlated on x and y axes, respectively. While SYN spectra are sensitive to simultaneous (in-phase) responses upon mechanical perturbation of functional groups attributed to specific vibrational bands, ASYN 2D-COS analysis enables the determination of out-of-phase responses and the order at which changes take place during damage repair. In this approach, positive cross-peaks (red) in SYN spectra represent simultaneous (both increase or decrease) changes in vibrational bands responsible for specific groups, whereas negative cross-peaks (blue) also indicate in-phase responses but in the opposite directions. On the other hand, positive cross-peaks (red) in ASYN spectra represent the responses of one band (wavenumber on the y axis—ν_2) before the other (wavenumber on the x axis—ν_1) and are out-of-phase, whereas negative cross-peaks (blue) are also due to sequential responses but in the opposite order.

Figure 2A2 illustrates SYN 2D-COS spectra of original p(AAEMA/MMA/nBA) CANs in the 1775−1560 cm^{-1}

https://doi.org/10.1021/acs.macromol.2c00739
Macromolecules 2022, 55, 4703−4709

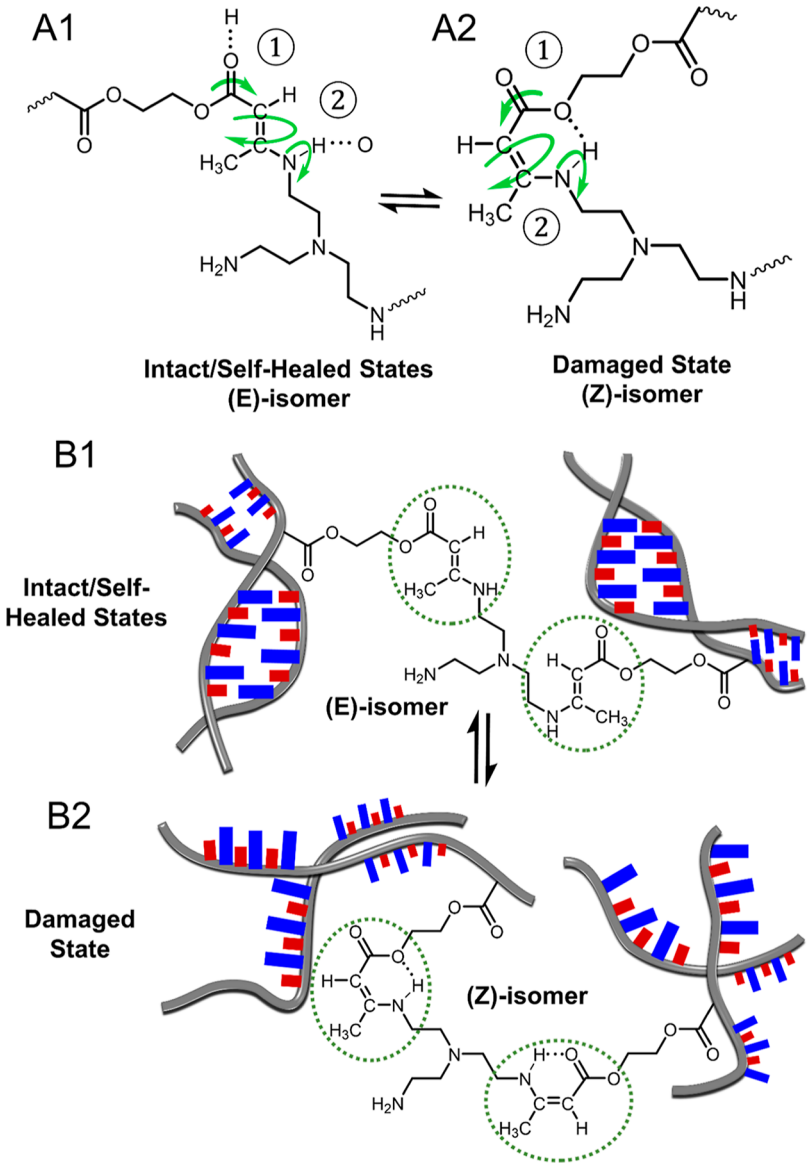

Figure 3. Molecular events during damage-repair cycle near tri-substituted C═C bonds in dynamic cross-links; (A1) intact/self-healed states: *E*-isomer; (A2) damaged state: unstable *Z*-isomer; (B1) intact/self-healed states of p(AAEMA/MMA/nBA) CANs; and (B2) damaged state of p(AAEMA/MMA/nBA) CANs.

region. The analysis of these data shows that upon damage, C═O groups of α, β unsaturated esters (1740 cm^{-1}) are in-phase with the C═C vibrations (1600 cm^{-1}) but respond in opposite directions, indicating symmetry and conformational changes in the vicinity of the C═C bond. The same response is observed for the C ═ O stretching band (1632 cm^{-1}) attributed to vinylogous urethane linkages in $R \times 4$ specimens (Figure 2B2). Because 2D-COS analysis enables not only the detection of molecular entities participating in the damage-repair cycle but also reveals the sequences of these events, Figure 2A3 shows that upon damage, the response of the C═C (1600 cm^{-1}) and N−H groups (1655 cm^{-1}) groups is asynchronous with respect to other C═O groups (1632, 1675, 1705, and 1740 cm^{-1}). This is also reflected in the slicing profile along the 1725 cm^{-1} band of the ASYN spectra shown in Figure 2A4. The positive directions (b, c, d, and f) of the C═O stretching in α,β unsaturated esters, H-bonded C═O groups, conjugated ketones, and the C═O in vinylogous urethanes indicate that the rearrangement of these entities occurs first. This is followed by the rotation of covalently attached C═C (a) and N−H (e) groups, as evidenced by the negative intensities of the respective bands (a) and (e) in Figure 2A4. As a result, the C═C bond undergoes rotation forming (*Z*) isomers. Both original (Figure 2A1−A4) and $R \times 4$ (Figure 2B1−B4) p(AAEMA/MMA/nBA) CANs exhibit the same responses to damage-repair perturbation.

Figure 3A summarizes sequential rearrangements within vinylogous urethane linkages during the damage-repair cycle. Upon mechanical damage (going from A1 to A2), inter-chain H-bonding of the C═O groups dissociates ①, followed by C═O groups' conformational rearrangements signified by arrows. Subsequently, the *E*-to-*Z* isomerization of the C═C bonds takes place, which parallels the response of the N−H groups ②. These sequential events lead to the dissociations of vdW interactions between neighboring chains, illustrated in Figure 3B1,B2. The C═C bonds of vinylogous urethane linkages (circled) prefer energetically favorable (*E*)-isomerization in the presence of inter-chain vdW interactions. Upon

https://doi.org/10.1021/acs.macromol.2c00739
Macromolecules 2022, 55, 4703−4709

self-healing, these events occur in the same order resulting in the recovery of vdW interactions between neighboring chains, inter- and intra-H-bonding, and (*Z*) ⇌ (*E*) isomerization around the C═C bond. It should be noted that substituents such as alkyl groups on amines and esters in vinylogous urethane moieties will increase the electron delocalization in unsaturated systems, thus promoting high electron densities on the carbonyl oxygen atom while reducing the C═O and C═C bond orders, which was reflected in spectroscopic analysis. This will result in H-bonding and the lower activation energy barrier to achieve the (*Z*) ⇌ (*E*) isomerization shown in Figure 3B, where dashed circles mark the location of this process. Also, the steric hindrance between ═C−CH_3 entities and N-alkyl groups linked to another chain in the (*Z*)-conformation upon damage will force N−H groups to bend toward COOR moieties, further strengthening intra-chain H-bonding. This, in turn, destabilizes the *Z*-conformations relative to the strainless *E* form, thus promoting self-healing.[33] Thermodynamically, conformational changes resulting in the movement of polymer chains are attributed to the amount of entropic energy stored during damage. Since entropic recovery is dependent on physical chain entanglements, self-healing driven by the entropy storage-recovery process and the regain of mechanical strength is manifested by chain movements.

CONCLUSIONS

In these studies, CANs that exhibit self-healing under ambient conditions and temperature/pressure reprocessing "built-in" into one copolymer network were developed. This was achieved by RAFT polymerization of AAEMA, MMA, and nBA monomers to yield a p(AAEMA/MMA/nBA) copolymer, which, upon cross-linking with TREN, formed autonomous self-healable and reprocessable [p(AAEMA/MMA/nBA)] CANs. These materials exhibit multiple self-healing cycles under ambient conditions and reprocessibility by compression molding at 120 °C. Notably, p(AAEMA/MMA/nBA) CANs showed significant enhancement of mechanical properties in relation to their thermoplastic p(MMA/nBA)[9] counterparts while retaining self-healing efficiency. The primary events responsible for reprocessing are associative transamination exchange reactions, which proceed through addition−elimination reactions of free primary amines reacting with vinylogous urethane *β*-carbons, releasing a new primary amine. Damage-repair cycles are dominated by the dissociation-reformation of vdW interactions and (*E*) ⇌ (*Z*) isomerization around C═C bonds. Upon mechanical damage, inter-chain H-bonding of the C═O groups dissociates, followed by C═O groups' conformational rearrangements. These sequential events lead to the dissociation of vdW interactions between neighboring chains. Upon self-healing, these events occur in the same order, resulting in the recovery of vdW interactions between neighboring chains, inter- and intra-H-bonding, and (*Z*) ⇌ (*E*) isomerization around the C═C bond. Although these studies represent one example of self-healable, reprocessable CANs, the availability of an array of exchange chemistries combined with self-healable commodity copolymers and equipped with ubiquitous vdWs interactions provides an opportunity for the development of new generations of self-healable and thermally reprocessable materials that can be technologically relevant and translate into technological opportunities.

ASSOCIATED CONTENT

Supporting Information

The Supporting Information is available free of charge at https://pubs.acs.org/doi/10.1021/acs.macromol.2c00739.

Experimental details, monomer synthesis, polymer synthesis, chemical and physical characterization (^{1}H NMR spectra and ATR FT-IR spectra), gel fraction, tensile tests, TGA, DMA, and GPC characterization (PDF)

AUTHOR INFORMATION

Corresponding Author

Marek W. Urban − *Department of Materials Science and Engineering, Clemson University, Clemson, South Carolina 29634, United States;* orcid.org/0000-0002-1522-2736; Email: mareku@clemson.edu

Authors

Siyang Wang − *Department of Materials Science and Engineering, Clemson University, Clemson, South Carolina 29634, United States*

Lei Li − *Department of Materials Science and Engineering, Clemson University, Clemson, South Carolina 29634, United States*

Qianhui Liu − *Department of Materials Science and Engineering, Clemson University, Clemson, South Carolina 29634, United States*

Complete contact information is available at: https://pubs.acs.org/10.1021/acs.macromol.2c00739

Notes

The authors declare no competing financial interest.

ACKNOWLEDGMENTS

This work was supported by the National Science Foundation under Awards DMR 2003005 and partially by OIA 1655740. The authors thank Kimberly Ivey for technical assistance in conducting thermogravimetric analysis as well as Tyler Reedy and Mastooreh Seyedi for their assistance in compression molding experiments.

REFERENCES

(1) Chen, X.; Dam, M. A.; Ono, K.; Mal, A.; Shen, H.; Nutt, S. R.; Sheran, K.; Wudl, F. A Thermally Re-mendable Cross-Linked Polymeric Material. *Science* **2002**, *295*, 1698−1702.

(2) Zhang, Y.; Broekhuis, A. A.; Picchioni, F. Thermally self-healing polymeric materials: the next step to recycling thermoset polymers? *Macromolecules* **2009**, *42*, 1906−1912.

(3) Yang, Y.; Urban, M. W. Self-Repairable Polyurethane Networks by Atmospheric Carbon Dioxide and Water. *Angew. Chem., Int. Ed.* **2014**, *53*, 12142−12147.

(4) Ghosh, B.; Urban, M. W. Self-repairing oxetane-substituted chitosan polyurethane networks. *Science* **2009**, *323*, 1458−1460.

(5) Imato, K.; Nishihara, M.; Kanehara, T.; Amamoto, Y.; Takahara, A.; Otsuka, H. Self-healing of chemical gels cross-linked by diarylbibenzofuranone-based trigger-free dynamic covalent bonds at room temperature. *Angew. Chem.* **2012**, *124*, 1164−1168.

(6) Cordier, P.; Tournilhac, F.; Soulié-Ziakovic, C.; Leibler, L. Self-healing and thermoreversible rubber from supramolecular assembly. *Nature* **2008**, *451*, 977−980.

(7) Holten-Andersen, N.; Harrington, M. J.; Birkedal, H.; Lee, B. P.; Messersmith, P. B.; Lee, K. Y. C.; Waite, J. H. pH-induced metal-ligand cross-links inspired by mussel yield self-healing polymer

networks with near-covalent elastic moduli. *Proc. Natl. Acad. Sci. U. S. A.* **2011**, *108*, 2651−2655.
(8) Burnworth, M.; Tang, L.; Kumpfer, J. R.; Duncan, A. J.; Beyer, F. L.; Fiore, G. L.; Rowan, S. J.; Weder, C. Optically healable supramolecular polymers. *Nature* **2011**, *472*, 334−337.
(9) Urban, M. W.; Davydovich, D.; Yang, Y.; Demir, T.; Zhang, Y.; Casabianca, L. Key-and-lock commodity self-healing copolymers. *Science* **2018**, *362*, 220−225.
(10) White, S. R.; Sottos, N. R.; Geubelle, P. H.; Moore, J. S.; Kessler, M. R.; Sriram, S. R.; Brown, E. N.; Viswanathan, S. Autonomic healing of polymer composites. *Nature* **2001**, *409*, 794.
(11) Corten, C. C.; Urban, M. W. Repairing polymers using oscillating magnetic field. *Adv. Mater.* **2009**, *21*, 5011−5015.
(12) Kloxin, C. J.; Scott, T. F.; Adzima, B. J.; Bowman, C. N. Covalent adaptable networks (CANs): a unique paradigm in cross-linked polymers. *Macromolecules* **2010**, *43*, 2643−2653.
(13) Denissen, W.; Rivero, G.; Nicolaÿ, R.; Leibler, L.; Winne, J. M.; Du Prez, F. E. Vinylogous urethane vitrimers. *Adv. Funct. Mater.* **2015**, *25*, 2451−2457.
(14) Podgórski, M.; Fairbanks, B. D.; Kirkpatrick, B. E.; McBride, M.; Martinez, A.; Dobson, A.; Bongiardina, N. J.; Bowman, C. N. Toward stimuli-responsive dynamic thermosets through continuous development and improvements in covalent adaptable networks (CANs). *Adv. Mater.* **2020**, *32*, No. e1906876.
(15) Montarnal, D.; Capelot, M.; Tournilhac, F.; Leibler, L. Silica-like malleable materials from permanent organic networks. *Science* **2011**, *334*, 965−968.
(16) Snyder, R. L.; Fortman, D. J.; De Hoe, G. X.; Hillmyer, M. A.; Dichtel, W. R. Reprocessable acid-degradable polycarbonate vitrimers. *Macromolecules* **2018**, *51*, 389−397.
(17) Fortman, D. J.; Brutman, J. P.; Cramer, C. J.; Hillmyer, M. A.; Dichtel, W. R. Mechanically activated, catalyst-free polyhydroxyurethane vitrimers. *J. Am. Chem. Soc.* **2015**, *137*, 14019−14022.
(18) Scott, T. F.; Schneider, A. D.; Cook, W. D.; Bowman, C. N. Photoinduced plasticity in cross-linked polymers. *Science* **2005**, *308*, 1615−1617.
(19) Cheng, K.; Chortos, A.; Lewis, J. A.; Clarke, D. R. Photoswitchable Covalent Adaptive Networks Based on Thiol−Ene Elastomers. *ACS Appl. Mater. Interfaces* **2022**, *14*, 4552−4561.
(20) Christensen, P. R.; Scheuermann, A. M.; Loeffler, K. E.; Helms, B. A. Closed-loop recycling of plastics enabled by dynamic covalent diketoenamine bonds. *Nat. Chem.* **2019**, *11*, 442−448.
(21) Chen, Q.; Yu, X.; Pei, Z.; Yang, Y.; Wei, Y.; Ji, Y. Multi-stimuli responsive and multi-functional oligoaniline-modified vitrimers. *Chem. Sci.* **2017**, *8*, 724−733.
(22) Bin Rusayyis, M. A.; Torkelson, J. M. Reprocessable covalent adaptable networks with excellent elevated-temperature creep resistance: facilitation by dynamic, dissociative bis (hindered amino) disulfide bonds. *Polym. Chem.* **2021**, *12*, 2760−2771.
(23) Chen, L.; Liu, R.; Hao, X.; Yan, Q. CO2-Cross-Linked Frustrated Lewis Networks as Gas-Regulated Dynamic Covalent Materials. *Angew. Chem., Int. Ed.* **2019**, *58*, 264−268.
(24) Solouki Bonab, V.; Karimkhani, V.; Manas-Zloczower, I. Ultra-Fast Microwave Assisted Self-Healing of Covalent Adaptive Polyurethane Networks with Carbon Nanotubes. *Macromol. Mater. Eng.* **2019**, *304*, 1800405.
(25) Lessard, J. J.; Garcia, L. F.; Easterling, C. P.; Sims, M. B.; Bentz, K. C.; Arencibia, S.; Savin, D. A.; Sumerlin, B. S. Catalyst-free vitrimers from vinyl polymers. *Macromolecules* **2019**, *52*, 2105−2111.
(26) Wang, S.; Urban, M. W. Self-Healable Fluorinated Copolymers Governed by Dipolar Interactions. *Adv. Sci.* **2021**, *8*, 2101399.
(27) Sosnowski, S.; Szymanski, R.; Lorandi, F.; Olszewski, M.; Sobieski, J.; Yin, R.; Bockstaller, M. R.; Matyjaszewski, K. Distribution of Alternating Sequences in Methyl Methacrylate/n-Butyl Acrylate Copolymers Prepared by Atom Transfer Radical Polymerization. *Macromolecules* **2021**, *54*, 9837−9849.
(28) Hornat, C. C.; Urban, M. W. Entropy and interfacial energy driven self-healable polymers. *Nat. Commun.* **2020**, *11*, 1028.
(29) Hornat, C. C.; Yang, Y.; Urban, M. W. Quantitative predictions of shape-memory effects in polymers. *Adv. Mater.* **2017**, *29*, 1603334.
(30) Bühringer, M. U.; Padberg, K.; Phleps, M. D.; Maid, H.; Placht, C.; Neiss, C.; Ferguson, M. J.; Goerling, A.; Tykwinski, R. R. Double bonds? Studies on the barrier to rotation about the cumulenic C=C bonds of tetraaryl [n] cumulenes (n= 3, 5, 7, 9). *Angew. Chem., Int. Ed.* **2018**, *57*, 8321−8325.
(31) Lasch, P.; Noda, I. Two-dimensional correlation spectroscopy (2D-COS) for analysis of spatially resolved vibrational spectra. *Appl. Spectrosc.* **2019**, *73*, 359−379.
(32) Šašić, S.; Ozaki, Y. Statistical two-dimensional correlation spectroscopy: Its theory and applications to sets of vibrational spectra. *Anal. Chem.* **2001**, *73*, 2294−2301.
(33) Gómez Sánchez, A.; Valle, A. M.; Bellanato, J. Infrared and nuclear magnetic resonance absorption and isomerism of 3-amino-crotonic esters. Part II. *J. Chem. Soc., Perkin Trans. 2* **1973**, 15−20.

https://doi.org/10.1021/acs.macromol.2c00739
Macromolecules 2022, 55, 4703−4709